scientific reports

Check for updates

OPEN

Delivery of the reduced form of vitamin $K_{2(20)}$ to NIH/3T3 cells partially protects against rotenone induced cell death

Erina Toki[1], Shotaro Goto[1], Shuichi Setoguchi[1], Kazuki Terada[2], Daisuke Watase[1], Hirofumi Yamakawa[3], Ayano Yamada[1], Mitsuhisa Koga[1], Kaori Kubota[1], Katsunori Iwasaki[1], Yoshiharu Karube[1], Kazuhisa Matsunaga[1]✉ & Jiro Takata[1]

Mitochondria generate energy through the action of the electron transport chain (ETC) and ATP synthase. Mitochondrial malfunction can lead to various disorders, including neurodegenerative diseases. Several reports have shown that menaquinone-4 (MK-4, vitamin $K_{2(20)}$), a safe drug for osteoporosis, may improve mitochondrial function. Here, we hypothesized that the efficient delivery of menahydroquinone-4 (MKH), an active form of MK-4, could exert a supporting effect. We verified the effects of MKH delivery on mitochondrial dysfunction by using MK-4 and MKH ester derivatives in NIH/3T3 mouse fibroblast cells treated with mitochondrial inhibitors. MK-4 and MKH derivatives suppressed cell death, the decline in mitochondrial membrane potential (MMP), excessive reactive oxygen species (ROS) production, and a decrease in intrinsic coenzyme Q_9 (CoQ_9) induced by rotenone (ROT, complex I inhibitor). MK-4 and MKH derivatives delivered MKH to NIH/3T3 cells, acting as an effective MKH prodrug, proving that the delivered MKH may reflect the mitigation effects on ROT-induced mitochondrial dysfunction. MKH prodrugs are also effective against 3-nitropropionic acid (3-NP, complex II inhibitor) and carbonyl cyanide-m-chlorophenylhydrazone (CCCP, uncoupler)-induced cell death. In conclusion, MKH delivery may mitigate mitochondrial dysfunction by maintaining MMP, ROS, and CoQ_9, indicating that MKH prodrugs may be good candidates for treating mitochondrial disorders.

Mitochondria are integral for normal cell functioning as they generate the ATP required to maintain vital cell function in the respiratory chain behaving as "powerhouses of the cell." Mitochondrial quality control and dysfunction are also implicated in the production of reactive oxygen species (ROS), regulation of cell death, and etiology of neurological disorders such as Huntington's disease, Parkinson's disease, and Alzheimer's disease[1–3]. Therefore, focusing on mitochondrial function is necessary to elucidate the etiology of diseases for which there are still no effective treatment strategies and advance effective drug development.

Mitochondria are organelles with a double-membrane structure containing five complexes in the inner membrane. In complexes I–IV (electron transport chain: ETC), protons are pumped into the intermembrane space during electron transport[4]. The concentration gradient of protons creates a mitochondrial membrane potential (MMP), which is used by complex V (ATP synthase) (Fig. 1). During the process of ATP production, the leaked electrons from the ETC generates ROS[5], while a reduced form of coenzyme Q (CoQ), known as a representative antioxidant in the ETC, protects against mitochondrial damage caused by ROS as a part of homeostasis mechanism. However, the production of excess ROS over the defense system in problematic situations causes oxidative stress and decreases membrane potential, resulting in an inability to produce energy and mitochondrial dysfunction[6]. Rotenone (ROT), a major complex I inhibitor, interferes with the conversion of CoQ to reduced CoQ ($CoQH_2$) by binding to NADH dehydrogenase, which is part of complex I[7,8]. As a result, electrons flow back, and ROS are generated, leading to cell death[9,10]. Therefore, ROT has been widely used in experimental models to explore drug effectiveness against mitochondrial dysfunction[11,12].

[1]Faculty of Pharmaceutical Sciences, Fukuoka University, Fukuoka 814-0180, Japan. [2]Faculty of Pharmaceutical Sciences, Himeji Dokkyo University, Himeji 670-8524, Japan. [3]Radioisotope Center, Fukuoka University, Fukuoka 814-0180, Japan. ✉email: k-matsu@fukuoka-u.ac.jp

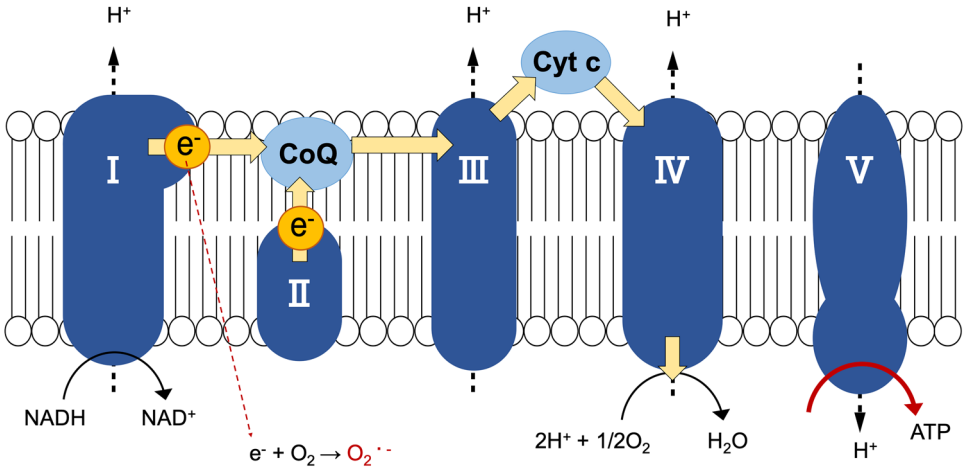

Figure 1. Mitochondrial respiratory chain complexes. Respiratory chain complexes I–IV generate a proton gradient on the mitochondrial inner membrane that facilitates ATP production by complex V (ATP synthase). The electron (e^-) passes through complex I and complex II, respectively, and moves to complex III via the CoQ. Cytochrome c (Cyt c) transfers an electron from complex III to complex IV, which reduces O_2 to form H_2O. Electron flow involves proton (H^+) transfer across the mitochondrial inner membrane at complexes I, III, and IV, creating an electrochemical gradient. Complex V uses the proton motive force to generate ATP.

Menaquinone-4 (MK-4, vitamin $K_{2(20)}$) has been clinically used as a therapeutic agent for osteoporosis in Japan, and its long-term safety has been confirmed[13]. It has been reported that MK-4 suppresses neuronal cell death mediated by ROT-induced microglial activation[14]. However, a recent study showed that vitamin K_2 is not a substitute for CoQ_{10}[15]. Other studies have reported that MK-4 can act as a mitochondrial electron transporter[16,17]. Thus, whether MK-4 is effective in mitochondrial dysfunction remains controversial. MK-4 cannot act as a cofactor for γ-glutamyl carboxylase (GGCX) for the post-translational modification of vitamin K-dependent proteins (VKDP) until MK-4 is reduced to menahydroquinone-4 (MKH)[18]. MKH is stoichiometrically converted to MK-4 epoxide (MKO) when it acts as a cofactor for GGCX (Fig. 2). Since MKH has a strong reduction capability, MKH but not MK-4 functions as a ROS scavenger. As a result, it would exert a protective effect against mitochondrial ROS. It has also been revealed that MKH is supplied not only by the reduction of exogenous MK-4 but also by biosynthesizing vitamin K_1 by UBIAD1[19] and has been reported to be highly distributed in the brain in the form of MK-4[20]. Therefore, if the efficacy of MK-4 is proven, it is speculated that our study will contribute to the development of safe and effective drugs for intractable diseases such as neurodegenerative disorders. However, MK-4 may not be well delivered to cells[21].

In our laboratory, we synthesized two MKH ester derivatives, MKH 1,4-bis-*N*,*N*-dimethylglycinate (MKH-DMG) and MKH 1,4-bis-hemi-succinate (MKH-SUC), which overcome the shortcomings of MK-4. In the present study, we aimed to verify whether MKH delivered by MKH prodrugs affected ROT-induced mitochondrial dysfunction and cell death. We have previously reported that MKH-DMG and MKH-SUC can act as effective MKH prodrugs in vitro and in vivo[21,22]. We have also shown that their MKH delivery via intracellular hydrolysis activation is independent of the reductive activation pathway for MK-4[23,24]. In this study, we evaluated the influence of MKH prodrugs on cell death, decrease in MMP, and intracellular CoQ levels following exposure to mitochondrial inhibitors, mainly ROT, in NIH/3T3 cells.

Results

MK-4 and MKH derivatives mitigate ROT-induced cell death. To verify whether MK-4 and MKH derivatives affect ROT (complex I inhibitor)-induced cell death in NIH/3T3 cells, cell viability was assessed using the CellTiter-Blue® (CTB, G8080, Promega Japan, Tokyo, Japan) reagent. As preliminary tests, the cytotoxicity of ROT, MK-4, or MKH derivatives to NIH/3T3 cells was evaluated. ROT treatment (0.01, 0.1, 1, and 10 μM for 24 h) induced a dose-dependent decrease in cell survival rate. The maximum reduction rate in cell viability was approximately 40% of the vehicle group (0.1% dimethylsulfoxide: DMSO) at the highest dose in the 0.01–10 μM dose range (Supplementary Fig. S1). In the absence of ROT, treatment with MK-4 and MKH derivatives for 24 h did not affect cell viability at concentrations of up to 3 μM (Supplementary Fig. S1). Based on the results of the preliminary cytotoxicity tests, the concentrations of the drug treatments were determined as follows: ROT, 10 μM; MK-4 and MKH derivatives, 0.03, 0.3, and 3 μM each. As shown in Fig. 3, the cell viability in the groups treated with MK-4 and MKH derivatives at 0.3 and 3 μM was higher than that with ROT only, while 0.03 μM MK-4 and MKH derivatives did not affect ROT-induced cell death. At 0.3 μM the effects of MK-4 and MKH-SUC treatments reached a plateau, while that of MKH-DMG treatments peaked at 3 μM (Fig. 3). These results showed that the MK-4 and MKH derivatives mitigated ROT-induced cell death.

MK-4 and MKH derivatives alleviate ROT-induced dysfunction of mitochondria. To observe the mitochondrial state before ROT-induced cell death occurs, MMP was evaluated by JC-1 staining. The changes

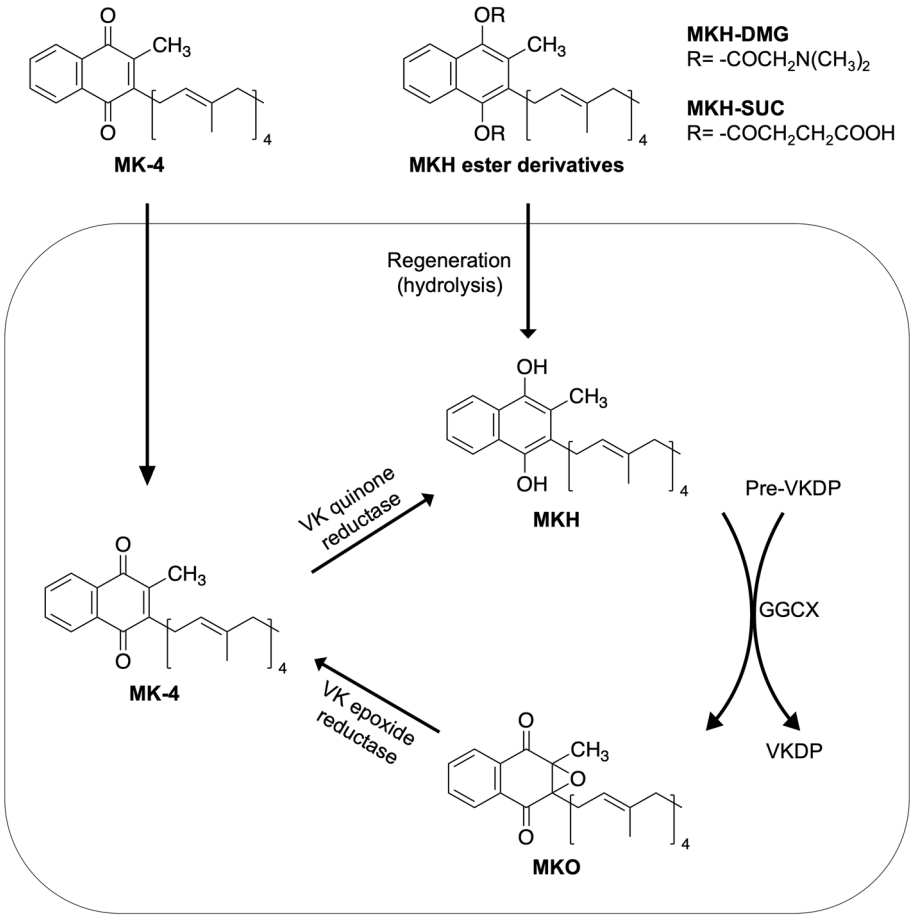

Figure 2. Schematic illustration of the vitamin K cycle and concept of the menahydroquinone-4 delivery system. MKH, menahydroquinone-4; MK-4, menaquinone-4; MKO, menaquinone-4 epoxide; VK, vitamin K; VKDP, vitamin K-dependent protein; GGCX, γ-glutamyl carboxylase.

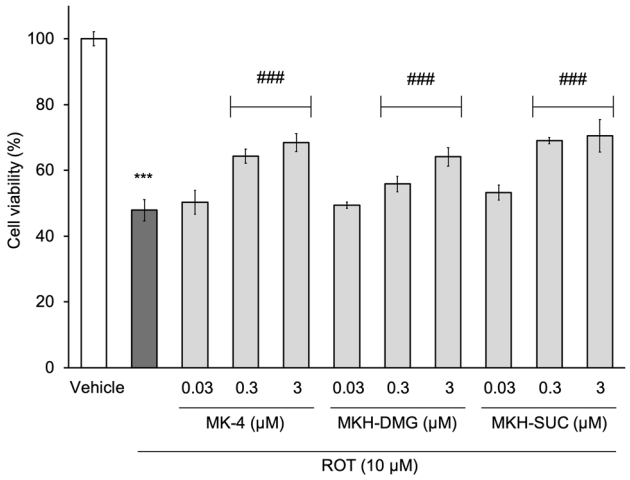

Figure 3. Influence of MK-4 and MKH derivatives on ROT-induced cell death. The NIH/3T3 cells were treated with 0.03−3 μM MK-4, MKH-DMG, or MKH-SUC for 24 h in the presence of 10 μM ROT. Cell viability was determined using the CTB assay. ***$p < 0.001$ versus vehicle group (0.1% DMSO + 0.1% ethanol); ###$p < 0.001$ versus ROT only group (Tukey's test). Mean ± SD (n = 3).

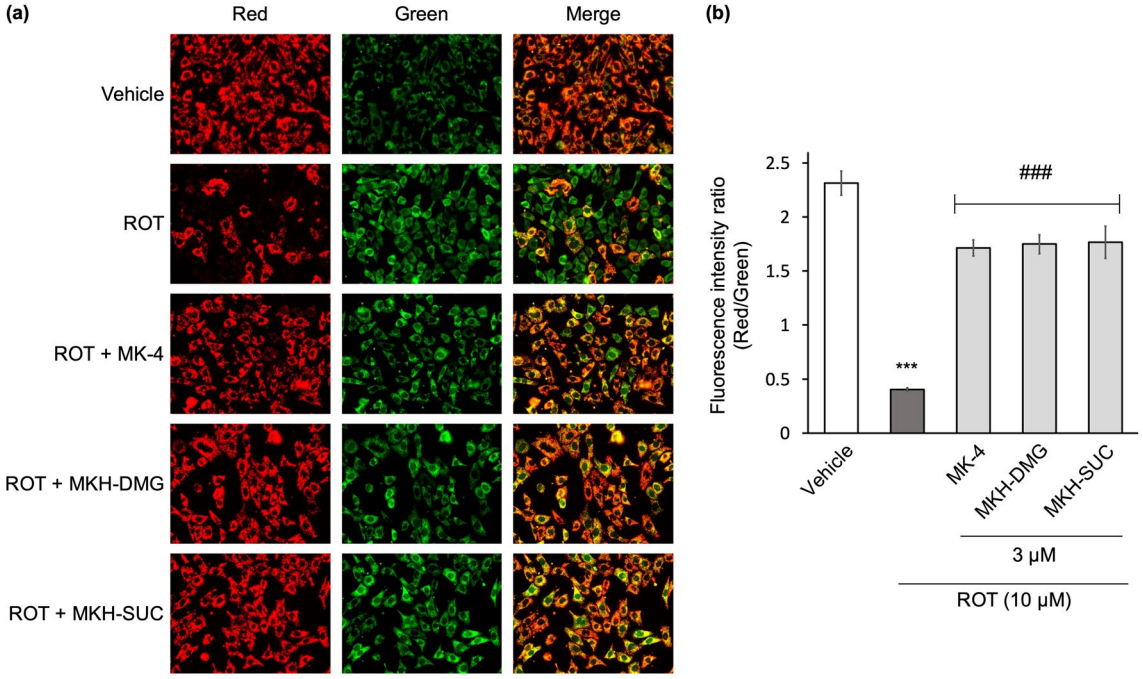

Figure 4. Influence of MK-4 and MKH derivatives on ROT-induced reduction of MMP. The NIH/3T3 cells were treated with 3 μM MK-4, MKH-DMG, or MKH-SUC for 6 h in the presence of 10 μM ROT. MMP was evaluated by JC-1 staining (**a**) Fluorescence microscopic image, (**b**) Fluorescence intensity ratio (Red/Green) quantified using a microplate reader. ***$p < 0.001$ versus vehicle group; ###$p < 0.001$ ROT only group (Tukey's test). Mean ± SD (n = 3).

in fluorescence from red to green of JC-1 showed a reduction in MMP. Treatment with 10 μM ROT for 6 h decreased the red fluorescence intensity compared to that in the vehicle group (0.1% DMSO + 0.1% ethanol), as shown in Fig. 4a. The red/green fluorescence intensity ratio was reduced by ROT, as shown in Fig. 4b, indicating mitochondrial dysfunction. Treatment with all three MK-4 and MKH derivatives alleviated the ROT-induced MMP reduction, as shown in Fig. 4a,b. These data indicated that MK-4 and MKH derivatives protected NIH/3T3 cells from ROT-induced mitochondrial damage.

MK-4 and MKH derivatives suppress ROT-induced ROS. ROT is believed to induce ROS in the mitochondria by blocking complex I in the respiratory chain. Therefore, to confirm the influence of MK-4 and MKH derivatives on ROT-induced ROS production, intracellular ROS levels were measured using 2′,7′-dichlorodihydrofluorescein diacetate (DCFH-DA) reagent. The intracellular ROS levels were standardized by the number of living cells, as indicated in Fig. 5. The ROS level in the ROT-only group was 1.7-fold higher than that in the vehicle group. In contrast, the levels of all three MK-4 and MKH derivatives were lower than those of the ROT-only group, indicating similar levels to that of the vehicle group. These data indicated that MK-4 and MKH derivatives maintained intracellular ROS levels in the normal state, even in the presence of ROT.

MK-4 and MKH derivatives suppress ROT-induced heme oxygenase-1 expression. Heme oxygenase-1 (HO-1) is induced by such as ROS and inflammatory cytokines. To evaluate the effect of ROT-induced ROS on the amount of HO-1 expression, real-time PCR and western blotting were performed. HO-1 gene expression increased eightfold in response to ROT compared to vehicle treatment (Fig. 6a). In contrast, the HO-1 gene expression levels of MK-4 and MKH derivatives were 2.7- to 4.0-fold lower than that of ROT (Fig. 6a). HO-1 protein expression was clearly increased by ROT, and the MK-4 and MKH derivatives suppressed ROT-induced HO-1 expression (Fig. 6b). The whole blot image can be found in Supplementary Figure S2. These data show that MK-4 and MKH derivatives suppress ROT-induced HO-1 gene and protein levels, supporting their suppressive effect on ROT-induced ROS.

MK-4 and MKH derivatives deliver MKH to NIH/3T3 and suppress ROT-induced coenzyme Q_9 decrease. To confirm MKH delivery by MK-4 and MKH derivatives and to investigate the effect of ROT-induced mitochondrial damage on the endogenous coenzyme Q_9 (CoQ_9)/reduced coenzyme Q_9 (CoQ_9H_2) balance, we measured intracellular MK-4, MKO, CoQ_9, and CoQ_9H_2 levels using LC–MS/MS. MKH cannot be measured directly because it is easily oxidized to MK-4 in presence of air. The MKO level reflects the amount of MKH delivered due to the conversion of MKH to MKO, which acts as a cofactor for the post-translational modification of VKDP by GGCX. In the vehicle group, neither MK-4 nor MKO was detected. Intracellular MKO was observed in the drug-treated groups, indicating that both the MK-4 and MKH derivatives functioned

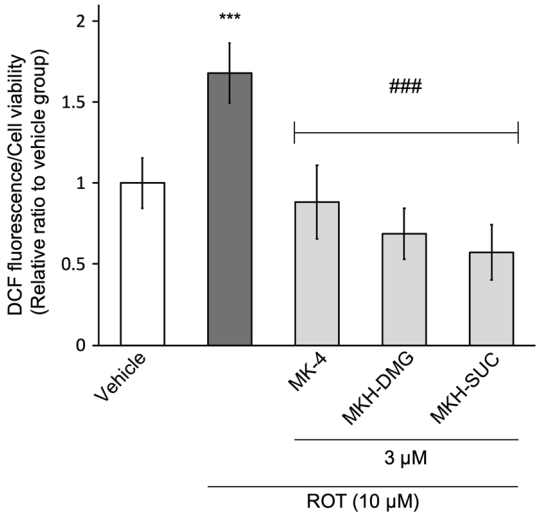

Figure 5. Influence of MK-4 and MKH derivatives on ROT-induced ROS. The NIH/3T3 cells were treated with 3 μM MK-4, MKH-DMG, or MKH-SUC for 6 h in the presence of 10 μM ROT. Intracellular ROS levels were determined by DCFH-DA staining. The relative luminescence unit (RLU) obtained using the DCFH-DA reagent was standardized by RLU from the CTB assay as the living cell number. ***$p < 0.001$ versus vehicle group; $^{###}p < 0.001$ versus ROT only group (Tukey's test). Mean ± SD (n = 3).

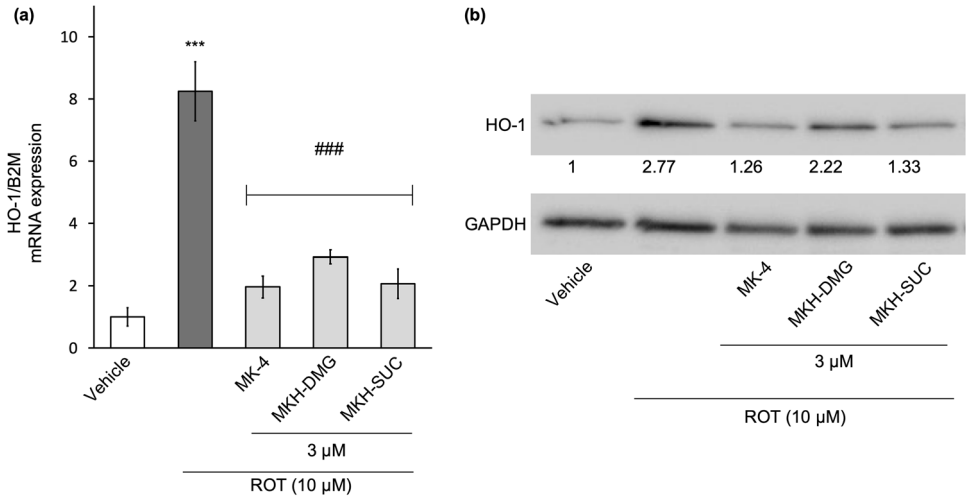

Figure 6. Influence of MK-4 and MKH derivatives on HO-1 induced by ROT. The NIH/3T3 cells were treated with 3 μM MK-4, MKH-DMG, or MKH-SUC for 6 h in the presence of 10 μM ROT. (**a**) HO-1 mRNA level obtained by qPCR. (**b**) HO-1 protein was detected by western blotting. ***$p < 0.001$ versus vehicle group; $^{###}p < 0.001$ versus ROT only group (Tukey's test). Data are presented as mean ± SD (n = 3).

as MKH prodrugs. After 6 and 24 h of drug treatment, intracellular MKO levels were higher than intracellular MK-4 levels at every time point. The maximum intracellular drug level of MK-4 was approximately 0.05 nmol/mg protein, and that of MKO was approximately 0.4 nmol/mg protein (Fig. 7a,b). These results suggested that the delivered MKH was efficiently utilized in the VKDP production process. The delivery of MKH by MK-4 and MKH derivatives was in the order MKH-SUC > MK-4 > MKH-DMG 6 h after drug treatment (Fig. 7a). After 24 h of treatment, the order of MKH delivery was MKH-DMG > MK-4 ≈ MKH-SUC (Fig. 7b). These results indicated that the ester hydrolysis of MKH-SUC in cells is fast, whereas that of MKH-DMG is steady.

In the CoQ_9H_2 measurement, a part of the CoQ_9H_2 was oxidized to CoQ_9 during the extraction process. Although oxidation could not be completely prevented, extraction was carried out promptly and simultaneously for all samples. The intracellular CoQ_9 level in the ROT-treated group at 6 h decreased compared to that in the vehicle group and reached 10% of the vehicle group after 24 h. Simultaneous treatment with MK-4 or MKH derivatives significantly suppressed the ROT-induced decrease in intracellular CoQ_9 level, which was about 70–90% of the vehicle group after 24 h (Fig. 7c,d). On the other hand, the amount of CoQ_9H_2 detected was approximately 5–10% of that of CoQ_9. ROT treatment markedly reduced CoQ_9H_2 after 6 h, but the MK-4 and MKH derivatives slightly affected the low levels of CoQ_9H_2 (Fig. 7e,f).

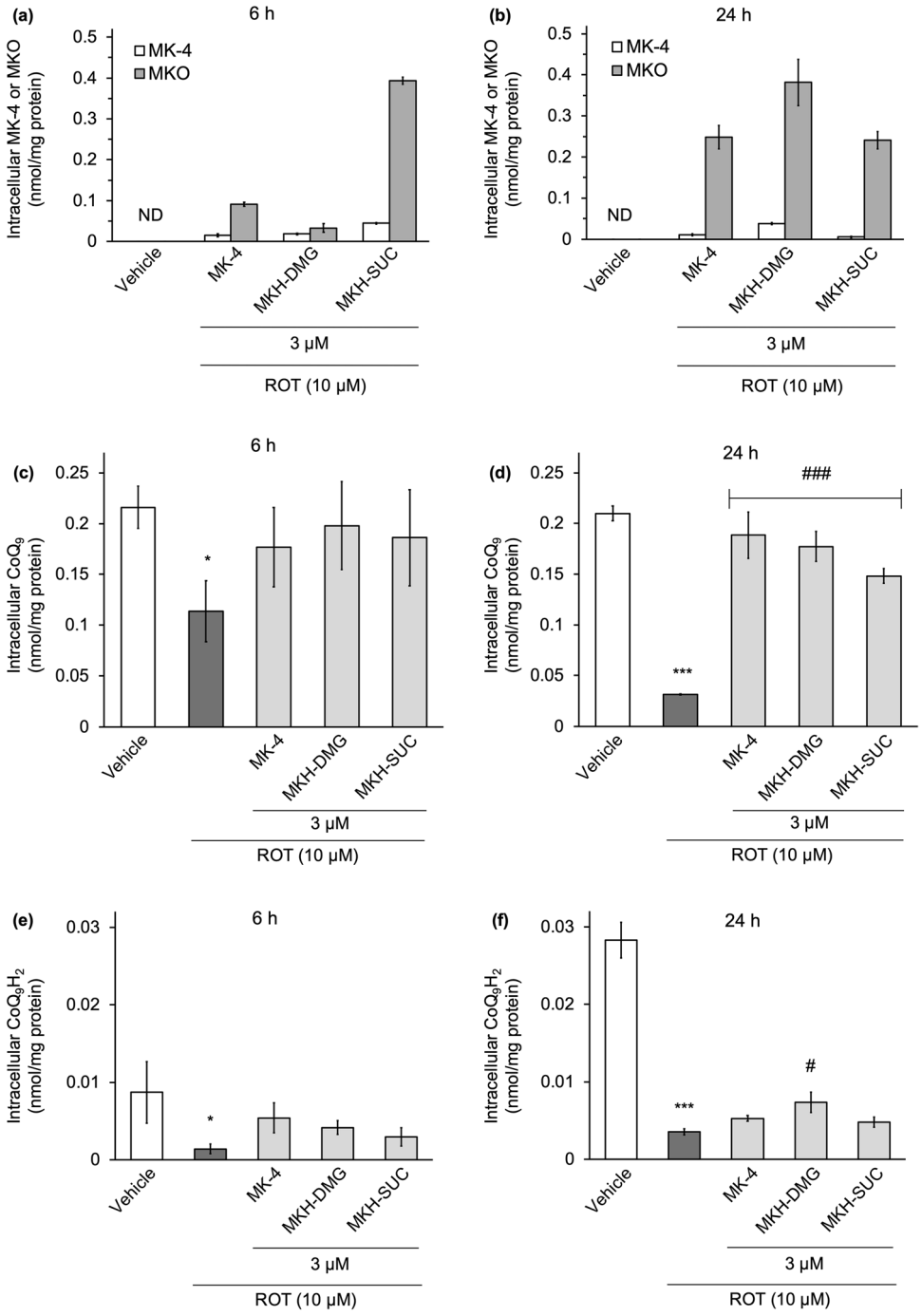

Figure 7. Intracellular MK-4, MKO, and native CoQ_9/CoQ_9H_2 levels in NIH/3T3 cells treated with ROT and MKH derivatives. The NIH/3T3 cells were treated with 3 μM MK-4, MKH-DMG, or MKH-SUC for 6 h or 24 h in the presence of 10 μM ROT. The intracellular levels of MK-4, MKO, CoQ_9, and CoQ_9H_2 were determined by LC–MS/MS. Intracellular MK-4 or MKO levels at (**a**) 6 h and (**b**) 24 h, CoQ_9 levels at (**c**) 6 h and (**d**) 24 h, CoQ_9H_2 levels at (**e**) 6 h and (**f**) 24 h. $^{***}p < 0.001$ versus vehicle group; $^{*}p < 0.05$ versus vehicle group; $^{\#\#\#}p < 0.001$ versus ROT only group; $^{\#}p < 0.05$ versus ROT only group (Tukey's test). Data are presented as mean ± SD (n = 3).

MK-4 and MKH derivatives protect against 3-NP- and CCCP-induced cell death but not against AA and OA. To elucidate the protective effects of MK-4 and MKH derivatives on other respiratory chain complex inhibitors; 3-nitro propionic acid (3-NP, complex II inhibitor), antimycin A (AA, complex III inhibitor), oligomycin A (OA, complex V inhibitor), and carbonyl cyanide m-chlorophenyl hydrazone (CCCP, uncoupler) were used. Cell viability was measured using CTB reagent, and the concentrations of all inhibitors used in the experiment were determined by preliminary experiments (Supplementary Fig. S3). Each of the inhibitors,

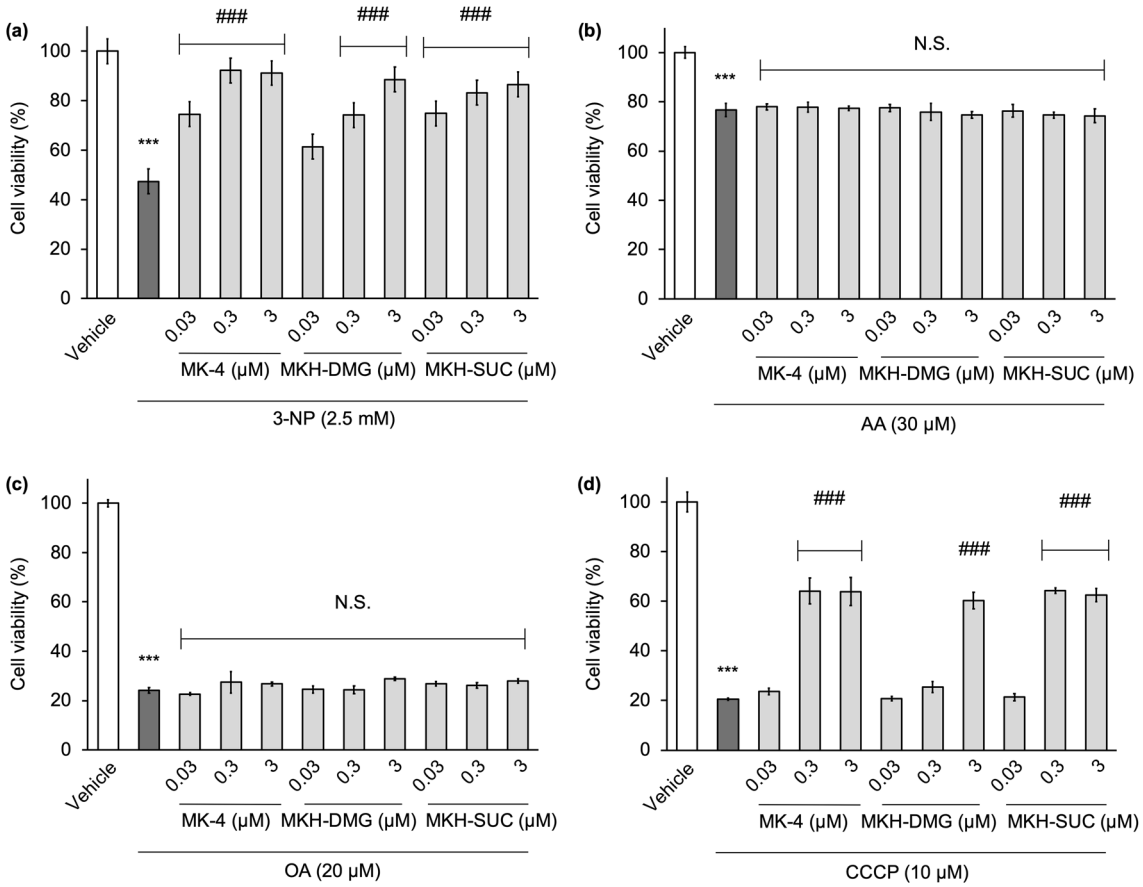

Figure 8. Influence of MK-4 and MKH derivatives on cell death induced by complex-II, III, V, and depolarization mitochondrial inhibitors. The NIH/3T3 cells were treated with 0.03−3 μM MK-4, MKH-DMG, or MKH-SUC for 24 h in the presence of (**a**) 2.5 mM 3-NP, (**b**) 30 μM AA, (**c**) 20 μM OA, and (**d**) 10 μM CCCP. Cell viability was determined using CTB assay. ***$p < 0.001$ versus vehicle group; ###$p < 0.001$ versus 3-NP only group or CCCP only group; no significant (N.S.) versus AA only group or OA only group (Tukey's test). Data are presented as mean ± SD (n = 3).

3-NP, AA, OA and CCCP, reduced the cell viability to 50%, 80%, 20%, and 20% of the vehicle group, respectively (0.1% ethanol) (Fig. 8). The MK-4 and MKH derivatives effectively mitigated the cytotoxicity of 3-NP and CCCP in a dose-dependent manner (Fig. 8a,d), whereas they did not affect AA- and OA-induced cell death (Fig. 8b,c).

Discussion

For vitamin K to exert pharmacological effects in post-translational modification of VKDP, antioxidation, and ROS scavenging, its naphthoquinone scaffold must be converted to naphthohydroquinone (a two-electron reduced form). It has been revealed that MKH (hydroquinone form of MK-4) is supplied not only by the reduction of exogenous MK-4 but also by biosynthesizing from vitamin K_1 by UBIAD1[19], and it has been reported that MKH is highly distributed in the brain in the form of MK-4[20]. To test the hypothesis of whether MKH is effective in mitochondrial dysfunction, which may correspond to various pathologies, such as Alzheimer's disease and Parkinson's disease, we investigated the effects of MK-4 and MKH derivatives as prodrugs of MKH on mitochondrial inhibitor-induced cytotoxicity in vitro. Vos et al. reported that MK-4 is responsible for ETC in Drosophila experiments[16]; however, Cerqua et al. showed that MK-4 is not a substitute for CoQ_{10} in mammalian cells[15]. Thus, whether MKH contributes to electron transport remains controversial.

NIH/3T3 cells are derived from mouse fibroblasts and are widely used for assessing basic biological effects such as cytotoxicity and elucidation of molecular mechanisms[25,26]. We employed NIH/3T3 cells to evaluate the essential effects of MKH derivatives on mitochondria. In his study, MK-4 and MKH derivatives showed a partial suppressive effect on NIH/3T3 cell death and mitochondrial dysfunction induced by mitochondrial inhibitors of complex I, II (ROT, 3-NP) and uncoupler (CCCP). Moreover, MK-4 and MKH derivatives acted as MKH prodrugs in NIH/3T3 cells and suppressed excessive ROS production and loss of endogenous CoQ_9 induced by ROT. Based on these results, it is speculated that MKH is a key player in mitigating mitochondrial dysfunction induced by mitochondrial inhibitors.

The effect and delivery of MKH-DMG were slower and milder than those of MK-4 and MKH-SUC (Figs. 3, 7a,b). Our previously published reports show a correlation between intracellular MKH delivery and efficacy, consistent with our results[23,24]. If MKH delivery is important for its suppressive effect on mitochondrial dysfunction,

it can be expected that the efficacy of MKH-DMG at low therapeutic concentrations will be lower than those of MK-4 and MKH-SUC. Therefore, it seems reasonable that the suppressive effects of MKH-DMG on the increase in cell death induced by mitochondrial inhibitors were lower than those of MK-4 and MKH-SUC (Figs. 3, 8a,d).

ROT treatment induced a significant decrease in MMP, increased ROS production, and increased HO-1 expression at early time points (Figs. 4, 5, 6). Xiong et al. showed that MMP reduction and ROS production occurred at an early stage after drug treatment, with ROS production occurring earlier[27]. Furthermore, Iacobini et al. suggest that ROT-induced ROS generation and MMP reduction are early events in cell death[28,29], and Geng et al. showed that short-term ROT treatment affected ROS production and MMP[30]. Therefore, our results indicated that the production of ROS induced a decrease in MMP, resulting in cell death. HO-1 is a stress response protein induced by oxidative stress, heavy metals, and cytokines, and exhibits cytoprotective and antioxidant activities[31,32]. ROS are representative factors that induce oxidative stress, and inhibition of ROS accumulation reduces HO-1 expression[33]. Thus, the level of HO-1 expression reflects the amount of ROS production. Our results showed that ROT exposes cells to stress (Fig. 6), and we speculate that it is because of ROS. MK-4 and MKH derivatives significantly suppressed the decrease in MMP, increase in ROS production and increase in HO-1 expression (Figs. 4, 5, 6). Therefore, we hypothesize that MK-4 and MKH derivatives relieved stress on cells by suppressing ROS overproduction, resulting in reduced MMP depletion and cell death.

CoQ_9 (oxidized form) and CoQ_9H_2 (two-electron reduced form) are electron transporters in the mitochondria, and CoQ_9 is more abundant than CoQ_{10} in rodents. NADH dehydrogenase in complex I activate the ETC by reducing CoQ_9–CoQ_9H_2. The MK-4 and MKH derivatives maintained endogenous CoQ_9 even in the presence of ROT (Fig. 7c,d). The ratio of CoQ_9H_2/CoQ_9 in NIH/3T3 cells in the vehicle group was low (Fig. 7c,e). To our knowledge, although no data indicating the ratio in NIH/3T3 cells have been found, low ratios have been observed in certain tissues, excluding the liver, adipose, and plasma[34,35]. Previous reports have demonstrated that ROT, an NADH dehydrogenase inhibitor, increases the ratio of CoQ_9/CoQ_9H_2 within a short period of drug treatment[36,37]. In the present study, ROT treatment decreased not only CoQ_9H_2 (Fig. 7e,f) but also CoQ_9, particularly at 24 h (Fig. 7d), suggesting that the absolute amount of CoQ_9 was lost due to ROT-induced mitochondrial collapse. Remarkably, CoQ_9H_2 remained low despite the high CoQ_9 levels maintained by MK-4 and MKH derivatives (Fig. 7d,f). This result suggests that ROT strongly blocks the reduction of CoQ_9 to CoQ_9H_2 independent of normal CoQ_9 levels. In other words, MKH prodrugs may effectively suppress ROT-induced ROS production via (i) ROS quenching or (ii) electron transport in complex I instead of CoQ. Menke et al. reported the protective effect of CoQ_{10} on ROT-induced apoptosis in SH-SY5Y neuroblast cells, suggesting that excessive exogenous CoQ_{10} may overcome ROT inhibition via a bypass mechanism for the ETC[38].

It has been reported that the main sites of ROS generation in mitochondria are in complex I and III[39–41], particularly in complex I[42]. AA inhibits the reduction of CoQ in respiratory chain complex III and induces ROS production[43]. However, it has also been reported that ROS are generated not only in ETCs I and III but also in ETCs II and IV[44], 3-NP, which irreversibly inhibits succinate dehydrogenase, generates ROS and promotes mitochondrial damage[45]. Furthermore, studies with CCCP, which reduces MMP and inhibits oxidative phosphorylation, and OA, which binds to the proton pump of complex V and inhibits ATP synthesis, confirm ROS generation[46,47]. Regarding the inhibitory effect of MK-4 and MKH derivatives on cell death induced by 3-NP and CCCP, it is necessary to further investigate whether the effects of MKH prodrug are due to the normalization of ROS levels and ROT. However, it is unclear why MK-4 and MKH derivatives have no effect on OA- and AA-induced cell death. Although Cerqua et al. showed that MK-4 does not function as a substitute for CoQ by using CoQ-depleted cells, the ROT used in our study did not block CoQ biosynthesis and did not lead to CoQ depletion in the mitochondria[15]. Therefore, MKH may be able to assist or substitute for CoQ to drive the ETC. Another possibility is that the increased MKO levels by MKH prodrugs reflect the production of VKDP, and induced VKDP may affect mitochondrial rescue. Further clarification of the mechanisms underlying the suppressive effects of MKH prodrugs on mitochondrial dysfunction, including the mechanism by which MKH prodrugs maintain ROS at normal levels, is required.

In this study, we present the basic effects of MKH derivatives on mitochondrial dysfunction and confirmed reproducibility. MK-4 and MKH derivatives have a partial inhibitory effect on cell death induced by respiratory chain complex I and II inhibitors and uncouplers and suppress ROS generation in mitochondria. These compounds functioned as prodrugs of MKH in NIH/3T3 cells, and it was considered that MKH delivery exerts a suppressive effect on cell death and ROS production. It is believed that the evaluation of the effect of MKH prodrugs on mitochondrial dysfunction and elucidation of the detailed mechanism using NIH/3T3 cells will become a foundation for further developmental research using cells derived from various organs.

Materials and methods

Chemicals. Menaquinone-4 (MK-4) was purchased from Seebio Biotech Inc. (Shanghai, China). Menahydroquinone-4 1,4-bis-*N*,*N*-dimethylglycinate hydrochloride (MKH-DMG), and menahydroquinone-4 1,4-bis-hemi-succinate (MKH-SUC) were synthesized in our laboratory using previously reported methods[48]. The following chemicals were obtained commercially: rotenone (R8875), 3-nitropropionic acid (N5636), and antimycin A from *Streptomyces* sp. (A8674) from Sigma-Aldrich (St. Louis, MO, USA); oligomycin A (AG-CN2-0517) from AdipoGen Life Sciences, Inc. (San Diego, CA, US); carbonyl cyanide m-chlorophenylhydrazone (CCCP; 034-16993) from FUJIFILM Wako Pure Chemical Corporation (Osaka, Japan); and coenzyme Q_9 (CoQ_9) from Cayman Chemical (Ann Arbor, MI, USA). The following antibodies were used: heme oxygenase 1 (HO-1) from Cell Signaling Technology (Danvers, MA, USA) and monoclonal mouse anti-glyceraldehyde-3-phosphate dehydrogenase (GAPDH) from Sigma-Aldrich.

Cell culture. The mouse fibroblast-like cell line NIH/3T3 (RCB2767) was obtained from the RIKEN BioResource Research Center (Ibaraki, Japan). Cells were maintained in Dulbecco's Modified Eagle Medium/Nutrient Mixture F-12 (DMEM/F-12; Thermo Fisher Scientific, Waltham, MA, USA) containing 10% fetal bovine serum (FBS; HyClone Standard Fetal Bovine Serum Collected and Processed in USA, Cytiva, Tokyo, Japan) and 1% penicillin/streptomycin (Thermo Fisher Scientific) at 37 °C under humidified 5% CO_2 atmosphere.

Cell viability assay. Cell viability was assessed using the CellTiter-Blue® (CTB, Promega) by the following cell viability assay method. NIH/3T3 cells were plated at a density of 1.0×10^4 cells per well in 96-well black plates and allowed to attach for 24 h. Then, drug media, including 10 μM of ROT and 0.03−3 μM of MK-4, MKH-DMG, or MKH-SUC at the different concentrations indicated in the related result section, were exposed for 24 h. Fluorescence signals as cell viability were measured using a microplate reader (Infinite M200 PRO, Tecan, Kanagawa, Japan) according to the manufacturer's instructions.

Measurement of the mitochondrial membrane potential. MMP in cells was assessed using the JC-1 MitoMP Detection Kit (Dojindo Lab, Kumamoto, Japan) according to the manufacturer's instructions. JC-1 accumulated in mitochondria forms red fluorescent aggregates at high membrane potentials, whereas JC-1 monomers show green fluorescence, indicating low membrane potentials. For the analysis of MMP, NIH/3T3 cells were cultured in a collagen-I-coated 96-well black plate at a density of 1.0×10^4 cells/well or in a collagen-I-coated glass dish (IWAKI, AGC TECHNO GLASS Co. Ltd, Shizuoka, Japan) at a density of 2.5×10^5 cells/dish. The cells were allowed to adhere for 24 h. The cells were then treated with MK-4, MKH-DMG, or MKH-SUC in the presence of ROT for 6 h. Then, the cells were stained with JC-1 (1 mg/mL in DMSO) and incubated at 37 °C for 30 min in the dark. The cells were washed twice with serum-free media, visualized under a fluorescence microscope (BZ-X810, KEYENCE, Osaka, Japan), and quantified using a microplate reader (Infinite M200 PRO) (red; Ex/Em = 561/595 nm, green; Ex/Em = 488/540 nm).

Intracellular ROS measurement. Intracellular ROS levels were examined using DCFH-DA (Thermo Fisher Scientific). The DCFH-DA probe is rapidly oxidized by ROS and converted into fluorescent 2′,7′-dichlorodihydrofluorescein (DCF). The DCF fluorescence intensity is proportional to the ROS level in the cytoplasm. Briefly, NIH/3T3 cells were seeded at a density of 1.0×10^4 cells/well in a collagen-I-coated 96-well black plate and allowed to adhere for 24 h. The cells were treated with MK-4, MKH-DMG, or MKH-SUC in the presence of ROT for 6 h. The cells were washed once with serum-free media and incubated in 100 μL of 10 μM DCFH-DA for 30 min in the dark at 37 °C. After incubation, intracellular fluorescence was measured at excitation and emission wavelengths of 485 and 530 nm, respectively, using a microplate reader (Infinite M200 PRO). The obtained ROS levels were standardized by cell viability using the CTB reagent, as described in the Cell Viability Assay section.

Real-time quantitative PCR. Total RNA was extracted from cultured cells using a High Pure RNA Isolation Kit (Roche Diagnostics K.K., Tokyo, Japan). cDNA was reverse-transcribed using the ReverTra Ace-a-reverse transcription kit (Toyobo, Shanghai, China), and quantification was performed using LightCycler® 480 SYBR Green I Master (Roche Diagnostics K.K.). The sequences of the primers used were as follows: heme oxygenase-1 (HO-1), forward primer: 5′-CACTCTGGAGATGACACCTGAG-3′; reverse primer: 5′- GTGTTC CTCTGTCAGCATCACC-3′; beta-2 microglobulin (B2M), forward primer: 5′- ACGTAGCAGTTCAGTATG TTCG-3′; reverse primer: 5′- GGTCTTTCTGGTGCTTGTCT-3′. B2M was used as an internal control.

Western blot analysis. NIH/3T3 cells were seeded at a density of 4.0×10^5 cells/dish in a collagen-I coated 60 mm dish and treated with 10 μM ROT with or without 3 μM MK-4, MKH-DMG, or MKH-SUC for 6 h. Cultured cells were washed with ice-cold PBS and lysed in RIPA buffer (0.5% NP-40, 0.25% sodium deoxycholate, 0.05% SDS, 150 mM NaCl, and 50 mM HEPES, pH 7.4) containing a protease inhibitor cocktail (Nacalai Tesque, Kyoto, Japan) on ice. A plastic cell scraper was used to scrape the adherent cells. Cell lysates were then clarified by centrifugation at $20{,}600 \times g$ at 4 °C for 15 min, and the supernatant was collected. The total protein concentration was determined using the Pierce™ BCA protein assay kit (Thermo Fisher Scientific). Proteins (every 10 μg) were separated by SDS-PAGE using Super Sep ™ Ace 15% 13-well gels (FUJIFILM Wako) and transferred onto PVDF membranes (Bio-Rad, Hercules, CA, USA). The membrane was blocked using Blocking One solution (Nacalai Tesque) and incubated with anti-HO-1 (1:1,000) and anti-GAPDH antibodies (1:10,000), respectively, at 25 °C for 1 h. After washing, the membranes were treated with the appropriate secondary antibodies and visualized using Immunostar LD (FUJIFILM Wako). Protein expression was analyzed using the ImageJ software (version 1.53 k).

Determination of intracellular MKO, MK-4, CoQ_9, and CoQ_9H_2. NIH/3T3 cells were seeded at 3.0×10^5 cells/well in 6-well plates and allowed to attach for 24 h. Next, the cells were cultured in a medium with or without 3 μM MK-4, MKH-DMG, or MKH-SUC in the presence of 10 μM ROT. The medium was then removed, and the cells were washed twice with PBS. The cells were collected in 1 mL PBS and sonicated on ice. Cell homogenates were combined with an equal volume of ethanol and three times the volume of n-hexane, vortexed for 2 min, and centrifuged at $1750 \times g$ for 10 min. The organic layer was evaporated using N_2 gas. The residue was reconstituted with 200 μL of ethanol and analyzed using LC–MS/MS, as described below. The protein concentration in the cell homogenate was determined using a BCA protein assay kit (Thermo Fisher Scientific).

LC–MS/MS. LC–MS/MS was performed using an LC–MS-8060 liquid chromatography-mass spectrometer (Shimadzu, Kyoto, Japan) and a Shimadzu UFLC System (Shimadzu, Kyoto, Japan). Separations were performed on a Shim-pack XR-C8 column (φ 2.2 μm, 3 × 75 mm, Shimadzu) using a mobile phase comprising 10 mM ammonium acetate and 0.1% acetic acid in methanol (pump A) and ethanol (pump B) under gradient elution, at a flow rate of 0.2 mL/min. A binary gradient was established as follows: (A) 10 mM ammonium acetate and 0.1% acetic acid in methanol and (B) 10 mM ammonium acetate and 0.1% acetic acid in ethanol; 30% B at 0 min, 30% B at 2.00 min, 70% B at 10.00 min, 70% B at 10.01 min, and 70% B at 12.00 min. The column temperature was maintained at 40 °C. The mass spectrometer was equipped with an electrospray ionizer and operated in the positive ion mode. Identification and quantitation were performed under the MS/MS-multiple reaction monitoring (MRM) mode, using the following transition ions: m/z 461.0 → 81.0 for the $[M+H]^+$ MKO adduct; m/z 445.0 → 187.0, for the $[M+H]^+$ MK-4 adduct; m/z 815.2 → 197.0, for the $[M+NH_4]^+$ CoQ_9H_2 adduct; and m/z 796.2 → 197.0, for the $[M+H]^+$ CoQ_9 adduct. Retention times were as follows: MKO, 3.5 min; MK-4, 3.9 min; CoQ_9H_2, 5.5 min; and CoQ_9, 7.4 min.

Statistical analysis. Comparisons among groups were performed by one-way ANOVA with Tukey's test, and the analyses were carried out using GraphPad Prism 6 (GraphPad Software, San Diego, CA, USA); results with $p < 0.05$ were considered significant.

Data availability

The datasets generated during and/or analyzed during the current study are available from the corresponding author upon reasonable request.

Received: 23 August 2022; Accepted: 15 November 2022
Published online: 18 November 2022

References

1. Damiano, M., Galvan, L., Deglon, N. & Brouillet, E. Mitochondria in Huntington's disease. *BBA-Mol. Basis Dis.* **52–61**, 2010. https://doi.org/10.1016/j.bbadis.2009.07.012 (1802).
2. Henchcliffe, C. & Beal, M. F. Mitochondrial biology and oxidative stress in Parkinson disease pathogenesis. *Nat. Clin. Pract. Neurol.* **4**, 600–609. https://doi.org/10.1038/ncpneuro0924 (2008).
3. Yan, M. H., Wang, X. L. & Zhu, X. W. Mitochondrial defects and oxidative stress in Alzheimer disease and Parkinson disease. *Free Radical Biol. Med.* **62**, 90–101. https://doi.org/10.1016/j.freeradbiomed.2012.11.014 (2013).
4. Zorova, L. D. *et al.* Mitochondrial membrane potential. *Anal. Biochem.* **552**, 50–59. https://doi.org/10.1016/j.ab.2017.07.009 (2018).
5. Wang, W. *et al.* Superoxide flashes in single mitochondria. *Cell* **134**, 279–290. https://doi.org/10.1016/j.cell.2008.06.017 (2008).
6. Sanderson, T. H., Reynolds, C. A., Kumar, R., Przyklenk, K. & Huttemann, M. Molecular mechanisms of ischemia-reperfusion injury in brain: Pivotal role of the mitochondrial membrane potential in reactive oxygen species generation. *Mol. Neurobiol.* **47**, 9–23. https://doi.org/10.1007/s12035-012-8344-z (2013).
7. Singer, T. P. & Ramsay, R. R. The reaction sites of rotenone and ubiquinone with mitochondrial nadh dehydrogenase. *BBA Bioenergetics* **1187**, 198–202. https://doi.org/10.1016/0005-2728(94)90110-4 (1994).
8. Braun, H. P. & Zabaleta, E. Carbonic anhydrase subunits of the mitochondrial NADH dehydrogenase complex (complex I) in plants. *Physiol. Plant.* **129**, 114–122. https://doi.org/10.1111/j.1399-3054.2006.00773.x (2007).
9. Mao, Y. R., Jiang, L., Duan, Y. L., An, L. J. & Jiang, B. Efficacy of catalpol as protectant against oxidative stress and mitochondrial dysfunction on rotenone-induced toxicity in mice brain. *Environ. Toxicol. Pharmacol.* **23**, 314–318. https://doi.org/10.1016/j.etap.2006.11.012 (2007).
10. Condello, S. *et al.* Agmatine effects on mitochondrial membrane potential and NF-kappa B activation protect against rotenone-induced cell damage in human neuronal-like SH-SY5Y cells. *J. Neurochem.* **116**, 67–75. https://doi.org/10.1111/j.1471-4159.2010.07085.x (2011).
11. Sanders, L. H. & Greenamyre, J. T. Oxidative damage to macromolecules in human Parkinson disease and the rotenone model. *Free Radical Biol. Med.* **62**, 111–120. https://doi.org/10.1016/j.freeradbiomed.2013.01.003 (2013).
12. Habib, C. N. *et al.* The potential neuroprotective effect of diosmin in rotenone-induced model of Parkinson's disease in rats. *Eur. J. Pharmacol.* https://doi.org/10.1016/j.ejphar.2021.174573 (2022).
13. Orimo, H. *et al.* Effects of menatetrenone on the bone and calcium metabolism in osteoporosis: A double-blind placebo-controlled study. *J. Bone Miner. Metab.* **16**, 106–112. https://doi.org/10.1007/s007740050034 (1998).
14. Yu, Y. X. *et al.* Vitamin K-2 suppresses rotenone-induced microglial activation in vitro. *Acta Pharmacol. Sin.* **37**, 1178–1189. https://doi.org/10.1038/aps.2016.68 (2016).
15. Cerqua, C. *et al.* Vitamin K2 cannot substitute Coenzyme Q(10) as electron carrier in the mitochondrial respiratory chain of mammalian cells. *Sci. Rep.* https://doi.org/10.1038/s41598-019-43014-y (2019).
16. Vos, M. *et al.* Vitamin K2 is a mitochondrial electron carrier that rescues pink1 deficiency. *Science* **336**, 1306–1310. https://doi.org/10.1126/science.1218632 (2012).
17. Bhalerao, S. & Clandinin, T. R. Vitamin K-2 takes charge. *Science* **336**, 1241–1242. https://doi.org/10.1126/science.1223812 (2012).
18. Tie, J. K. & Stafford, D. W. Structural and functional insights into enzymes of the vitamin K cycle. *J. Thromb. Haemost.* **14**, 236–247. https://doi.org/10.1111/jth.13217 (2016).
19. Nakagawa, K. *et al.* Identification of UBIAD1 as a novel human menaquinone-4 biosynthetic enzyme. *Nature* **468**, 117. https://doi.org/10.1038/nature09464 (2010).
20. Carrie, I. *et al.* Menaquinone-4 concentration is correlated with sphingolipid concentrations in rat brain. *J. Nutr.* **134**, 167–172. https://doi.org/10.1093/jn/134.1.167 (2004).
21. Setoguchi, S. *et al.* Enhanced antitumor effects of novel intracellular delivery of an active form of menaquinone-4, menahydroquinone-4, into hepatocellular carcinoma. *Cancer Prev. Res.* **8**, 129–138. https://doi.org/10.1158/1940-6207.capr-14-0292 (2015).
22. Setoguchi, S. *et al.* Antitumor effects and delivery profiles of menahydroquinone-4 prodrugs with ionic or nonionic promoiety to hepatocellular carcinoma cells. *Molecules.* https://doi.org/10.3390/molecules23071738 (2018).
23. Yamakawa, H. *et al.* Growth inhibitory effects of ester derivatives of menahydroquinone-4, the reduced form of vitamin K-2(20), on all-trans retinoic acid-resistant HL60 cell line. *Pharmaceutics.* https://doi.org/10.3390/pharmaceutics13050758 (2021).
24. Goto, S. *et al.* Prodrugs for skin delivery of menahydroquinone-4, an active form of vitamin K-2(20), could overcome the photoinstability and phototoxicity of vitamin K-2(20). *Int. J. Mol. Sci.* https://doi.org/10.3390/ijms20102548 (2019).

25. Ayaz, M. *et al.* Molecularly characterized solvent extracts and saponins from *Polygonum hydropiper* L. show high anti-angiogenic, anti-tumor, brine shrimp, and fibroblast NIH/3T3 cell line cytotoxicity. *Front. Pharmacol.* https://doi.org/10.7789/fphar.2016.00074 (2016).
26. Hsin, Y. H. *et al.* The apoptotic effect of nanosilver is mediated by a ROS- and JNK-dependent mechanism involving the mitochondrial pathway in NIH3T3 cells. *Toxicol. Lett.* **179**, 130–139. https://doi.org/10.1016/j.toxlet.2008.04.015 (2008).
27. Xiong, N. *et al.* The role of autophagy in Parkinson's disease: Rotenone-based modeling. *Behav. Brain Funct.* https://doi.org/10.1186/1744-9081-9-13 (2013).
28. Iacobini, M. *et al.* Involvement of oxygen radicals in cytarabine-induced apoptosis in human polymorphonuclear cells. *Biochem. Pharmacol.* **61**, 1033–1040. https://doi.org/10.1016/s0006-2952(01)00548-2 (2001).
29. Hwang, J. M., Cho, J. S., Kim, T. H. & Lee, Y. I. Ellagic acid protects hepatocytes from damage by inhibiting mitochondrial production of reactive oxygen species. *Biomed. Pharmacother.* **64**, 264–270. https://doi.org/10.1016/j.biopha.2009.06.013 (2010).
30. Geng, J. *et al.* Andrographolide alleviates Parkinsonism in MPTP-PD mice via targeting mitochondrial fission mediated by dynamin-related protein 1. *Br. J. Pharmacol.* **176**, 4574–4591. https://doi.org/10.1111/bph.14823 (2019).
31. Huang, J. Y. *et al.* 20C, a bibenzyl compound isolated from *Gastrodia elata*, protects PC12 cells against rotenone- induced apoptosis via activation of the Nrf2/ARE/HO-1 signaling pathway. *Acta Pharmacol. Sin.* **37**, 731–740. https://doi.org/10.1038/aps.2015.154 (2016).
32. Loboda, A., Damulewicz, M., Pyza, E., Jozkowicz, A. & Dulak, J. Role of Nrf2/HO-1 system in development, oxidative stress response and diseases: An evolutionarily conserved mechanism. *Cell. Mol. Life Sci.* **73**, 3221–3247. https://doi.org/10.1007/s00018-016-2223-0 (2016).
33. Fang, Y. K. *et al.* Activation of the ROS/HO-1/NQO1 signaling pathway contributes to the copper-induced oxidative stress and autophagy in duck renal tubular epithelial cells. *Sci. Total Environ.* https://doi.org/10.1016/j.scitotenv.2020.143753 (2021).
34. Matsura, T., Yamada, K. & Kawasaki, T. Changes in the content and intracellular-distribution of coenzyme-Q homologs in rabbit liver during growth. *Biochem. Biophys. Acta.* **1083**, 277–282. https://doi.org/10.1016/0005-2760(91)90083-t (1991).
35. Kishi, T., Takahashi, T., Usui, A., Hashizume, N. & Okamoto, T. Cytosolic NADPH-UQ reductase, the enzyme responsible for cellular ubiquinone redox cycle as an endogenous antioxidant in the rat liver. *BioFactors* **9**, 189–197. https://doi.org/10.1002/biof.5520090214 (1999).
36. Burger, N. *et al.* A sensitive mass spectrometric assay for mitochondrial CoQ pool redox state in vivo. *Free Radical Biol. Med.* **147**, 37–47. https://doi.org/10.1016/j.freeradbiomed.2019.11.028 (2020).
37. Galinier, A. *et al.* Biological validation of coenzyme Q redox state by HPLC-EC measurement: Relationship between coenzyme Q redox state and coenzyme Q content in rat tissues. *FEBS Lett.* **578**, 53–57. https://doi.org/10.1016/j.febslet.2004.10.067 (2004).
38. Menke, T. *et al.* Coenzyme Q(10) reduces the toxicity of rotenone in neuronal cultures by preserving the mitochondrial membrane potential. *BioFactors* **18**, 65–72. https://doi.org/10.1002/biof.5520180208 (2003).
39. Kudin, A. P., Bimpong-Buta, N. Y. B., Vielhaber, S., Elger, C. E. & Kunz, W. S. Characterization of superoxide-producing sites in isolated brain mitochondria. *J. Biol. Chem.* **279**, 4127–4135. https://doi.org/10.1074/jbc.M310341200 (2004).
40. Cadenas, E., Boveris, A., Ragan, C. I. & Stoppani, A. O. M. Production of superoxide radicals and hydrogen-peroxide by nadh-ubiquinone reductase and ubiquinol-cytochrome c reductase from beef-heart mitochondria. *Arch. Biochem. Biophys.* **180**, 248–257. https://doi.org/10.1016/0003-9861(77)90035-2 (1977).
41. Zhang, Q. *et al.* Involvement of ERK1/2 pathway in neuroprotective effects of pyrroloquinoline quinine against rotenone-induced SH-SY5Y cell injury. *Neuroscience* **270**, 183–191. https://doi.org/10.1016/j.neuroscience.2014.04.022 (2014).
42. Brand, M. D. The sites and topology of mitochondrial superoxide production. *Exp. Gerontol.* **45**, 466–472. https://doi.org/10.1016/j.exger.2010.01.003 (2010).
43. Chen, Q., Vazquez, E. J., Moghaddas, S., Hoppel, C. L. & Lesnefsky, E. J. Production of reactive oxygen species by mitochondria—Central role of complex III. *J. Biol. Chem.* **278**, 36027–36031. https://doi.org/10.1074/jbc.M304854200 (2003).
44. Zhao, R. Z., Jiang, S., Zhang, L. & Yu, Z. B. Mitochondrial electron transport chain, ROS generation and uncoupling (review). *Int. J. Mol. Med.* **44**, 3–15. https://doi.org/10.3892/ijmm.2019.4188 (2019).
45. Liot, G. *et al.* Complex II inhibition by 3-NP causes mitochondrial fragmentation and neuronal cell death via an NMDA- and ROS-dependent pathway. *Cell Death Differ.* **16**, 899–909. https://doi.org/10.1038/cdd.2009.22 (2009).
46. Vaamonde-Garcia, C. *et al.* The mitochondrial inhibitor oligomycin induces an inflammatory response in the rat knee joint. *BMC Musculoskelet. Disord.* https://doi.org/10.1186/s12891-017-1621-2 (2017).
47. Li, D. *et al.* Sulforaphane activates a lysosome-dependent transcriptional program to mitigate oxidative stress. *Autophagy* **17**, 872–887. https://doi.org/10.1080/15548627.2020.1739442 (2021).
48. Takata, J. *et al.* Vitamin-K prodrugs. 1. Synthesis of amino-acid esters of menahydroquinone-4 and enzymatic reconversion to an active form. *Pharm. Res.* **12**, 18–23 (1995).

Acknowledgements

We thank the students from our group, Natsumi Nishihara, Kayo Rikimaru, and Seiko Harada, for providing support with the execution of experiments in this study.

Author contributions

J.T. designed this research. E.T. performed the experiments with assistance from S.S., K.T., D.W., A.Y., M.K., and H.Y. Moreover, K.M., S.S., S.G., and E.T analyzed the data, E.T. wrote the manuscript, K.M., S.S., S.G, and K.K. helped with review and editing, Y.K., K.I., J.T., and K.M. oversaw the research. All the authors have approved the final version of the manuscript.

Competing interests

The authors declare no competing interests.

Additional information

Supplementary Information The online version contains supplementary material available at https://doi.org/10.1038/s41598-022-24456-3.

Correspondence and requests for materials should be addressed to K.M.